arXiv:cond-mat/0105465v1 [cond-mat.stat-mech] 23 May 2001

Finite-temperature simulations of the scissors mode in Bose-Einstein condensed gases

B. Jackson and E. Zaremba
Department of Physics, Queen's University, Kingston, Ontario K7L 3N6, Canada.
(February 1, 2008)

The dynamics of a trapped Bose-condensed gas at finite temperatures is described by a generalized Gross-Pitaevskii equation for the condensate order parameter and a semiclassical kinetic equation for the thermal cloud, solved using N-body simulations. The two components are coupled by mean fields as well as collisional processes that transfer atoms between the two. We use this scheme to investigate scissors modes in anisotropic traps as a function of temperature. Frequency shifts and damping rates of the condensate mode are extracted, and are found to be in good agreement with recent experiments.

PACS numbers: 03.75.Fi, 05.30.Jp, 67.40.Db

The experimental observation of the scissors mode in a gaseous Bose-Einstein condensate (BEC) [1] provided a characteristic signature of superfluidity in this system [2]. The scissors mode is excited by an angular displacement of the gas relative to an anisotropic confining potential. Above the BEC transition temperature, T_c, the resulting oscillation generally consists of the superposition of two modes, a high-frequency mode which reduces to an irrotational quadrupole mode in the limit of an isotropic trap, and a low-frequency mode which in the same limit corresponds to a pure rotation at zero frequency [2]. In contrast, a pure condensate exhibits only one oscillation frequency, indicating the irrotational, and therefore superfluid, nature of the gas. An important issue in superfluid systems is the transition between these regimes with increasing temperature. This question has recently been addressed experimentally for trapped gases [3], stimulating the need for a consistent theoretical description of the observed behavior.

It is well established that many properties of the condensate at very low temperatures can be described by the Gross-Pitaevskii (GP) equation [4], which is a nonlinear Schrödinger equation for the condensate wavefunction, $\Phi(\mathbf{r},t)$. The equation treats the condensate as a classical field and neglects quantum and thermal fluctuations. Consequently, the theory breaks down at higher temperatures ($T > 0.5T_c$) where the non-condensed component of the cloud is significant. Including the thermal component in a consistent manner is a considerable challenge. Most calculations, such as those based on the Hartree-Fock-Bogoliubov (HFB) equations [5,6], fail to capture the full collective dynamics of the thermal cloud, particularly its back-action on the condensate.

An approach which allows one to treat the dynamics of both components simultaneously was developed previously [7]. The resulting equations of motion reduce to a generalized GP equation for the condensate

$$i\hbar\frac{\partial}{\partial t}\Phi(\mathbf{r},t) = \Bigg(-\frac{\hbar^2}{2m}\nabla^2 + V(\mathbf{r}) + g[n_c(\mathbf{r},t) + 2\tilde{n}(\mathbf{r},t)] - iR(\mathbf{r},t)\Bigg)\Phi(\mathbf{r},t), \qquad (1)$$

and a semiclassical Boltzmann kinetic equation for the thermal cloud

$$\frac{\partial f}{\partial t} + \frac{\mathbf{p}}{m}\cdot\nabla f - \nabla U_{\rm eff}\cdot\nabla_{\mathbf{p}} f = C_{12}[f] + C_{22}[f]. \qquad (2)$$

$n_c(\mathbf{r},t) = |\Phi(\mathbf{r},t)|^2$ and $\tilde{n}(\mathbf{r},t)$ are the condensate and non-condensate densities, respectively, and the mean field acting on the thermal atoms is given by $U_{\rm eff} = V + 2g[n_c + \tilde{n}]$. Apart from mean field effects, Eqs. (1) and (2) are linked by the non-Hermitian source term, $R(\mathbf{r},t)$, which accounts for the transfer of atoms between the condensate and thermal cloud and is defined in terms of the $C_{12}[f]$ collision integral by

$$R(\mathbf{r},t) = \frac{\hbar}{2n_c}\int\frac{d\mathbf{p}}{(2\pi\hbar)^3}C_{12}[f]\,. \qquad (3)$$

In arriving at this set of equations, several approximations have been made. The use of a contact interatomic interaction, $g\delta(\mathbf{r}-\mathbf{r}')$ ($g = 4\pi\hbar^2 a/m$, where a is the atomic s-wave scattering length), is standard. More importantly, the thermal excitations are treated in the Hartree-Fock approximation. Furthermore, we invoke the Popov approximation, where the 'anomalous' density $\tilde{m}$ is neglected. This is in part motivated by physical concerns: inclusion of $\tilde{m}$ leads to unphysical low-momentum gaps in the energy spectrum, as well as infra-red and ultra-violet divergences. These inconsistencies can be removed either perturbatively [8], or through the use of refined kinetic equations [9]. The latter may provide a possible future extension of our work.

In this paper we apply the above set of equations to the calculation of the scissors mode in an anisotropic harmonic trap [$V(\mathbf{r}) = m(\omega_\rho^2\rho^2 + \omega_z^2 z^2)/2$] as a function of temperature for experimentally relevant parameters. The GP equation is solved using a FFT split-operator method [10], whereas the kinetic equation is solved by performing a classical simulation [11,12] in which the thermal phase-space density $f(\mathbf{p},\mathbf{r},t)$ is represented by an N-body system of discrete particles. Collisions between atoms are naturally treated in this representation

by Monte-Carlo computation of the C_{22} and C_{12} collision integrals. The complete dynamical problem becomes computationally feasible within this scheme, and has the additional advantage of providing an intuitive physical picture for the thermal gas dynamics. The damping rates and frequency shifts that we calculate for the scissors mode are in good agreement with experiment, indicating that our approach is valid over a wide range of temperatures. The simulations also yield the quadrupole response function of the system, which clearly illustrates the transition between superfluid and rigid-body behavior with increasing temperature.

Our simulations involve propagation over a sequence of time steps, Δt. The trajectories of the thermal atoms are obtained by solving Newton's equations of motion with forces defined by the mean field potential $U_{\rm eff}$. To ensure energy conservation the velocities and positions of the atoms are updated at each time-step using a second-order simplectic integrator [13]. To define the mean field of a thermal cloud consisting of discrete particles, we first allocate atoms to grid-points $\mathbf{r}_{jkl}$ using a cloud-in-cell approach [14], and then convolve this density distribution with a Gaussian function $G(\mathbf{r}) \sim e^{-r^2/\eta^2}$. This effectively is a smoothening procedure, which is equivalent to assuming that interactions involving thermal atoms have a finite range η. For consistency, the n_c term appearing in $U_{\rm eff}$ is also convolved.

The Monte-Carlo computation of the C_{22} collision term, describing collisions between two non-condensed atoms that both remain in the thermal cloud, was discussed in an earlier paper [15]. However, the C_{12} collision term, which transfers atoms between the two components, was neglected. We now include this term, but as the method is somewhat involved we will detail it elsewhere [16]. Briefly, one can write (3) as $R = R^{\rm in} - R^{\rm out}$, where $R^{\rm in}$ represents collisions between two thermal particles that lead to absorption of one by the condensate, while $R^{\rm out}$ refers to the inverse process. In terms of our Monte-Carlo simulations, one approximates the integrals by a sum over particles around a grid-point: $R(\mathbf{r}_{jkl},t) = (\hbar/2n_c)\sum_i \Delta P_i$, where $\Delta P_i = P_i^{\rm in} - P_i^{\rm out}$. The term $P_i^{\rm in}$ ($P_i^{\rm out}$) represents the probability that a given thermal atom with velocity $\mathbf{v}_i$ will collide during the time step, leading to a net transfer of particles in (out) of the condensate. Both probabilities are proportional to n_c and the Bose collision cross-section, $\sigma = 8\pi a^2$. They also depend upon the local condensate velocity $\mathbf{v}_c$ and the phase-space densities of the final thermal states, randomly selected to satisfy momentum and energy conservation.

In summary, the simulations consist of the following sequence. In a given time step, the thermal particle phase-space coordinates are first updated as discussed above. The probabilities of C_{12} collisions are next calculated for each atom. A random number $R \in [0,1]$ is chosen, and if $|\Delta P_i| > R$, atoms are added ($\Delta P_i < 0$) or removed ($\Delta P_i > 0$) appropriately. The quantity ΔP_i is also accumulated to define the dissipative term in (1). We then treat the C_{22} collisions [15]. Finally, the GP equation is propagated; the dissipative term, R, leads to a continuous change in normalization of the wavefunction which is consistent with the discrete addition or removal of particles from the thermal cloud.

Experimentally [1,3] the condensate is produced in a disk-shaped anisotropic trap ($\omega_z \sim \sqrt{8}\omega_\rho$), which is adiabatically tilted to make an angle θ_0 with respect to its original orientation. The scissors mode is then excited by suddenly switching the trap to an angle $-\theta_0$, so that the condensate and thermal cloud oscillate about this new equilibrium position. We simulate this scenario by first finding the equilibrium condensate and non-condensate density profiles for a particular temperature T using a self-consistent semiclassical procedure [15]. A sample of test particles is then chosen to simulate the phase space distribution, where to minimize statistical fluctuations, ten times the physical number of thermal atoms is used. Initial particle positions and momenta are randomly selected by a rejection method from a Bose distribution $f(\mathbf{p},\mathbf{r},t) = [z^{-1}\exp(\beta p^2/2m) - 1]^{-1}$, where $\beta \equiv 1/k_B T$ and $z(\mathbf{r}) = \exp(-\beta\{U_{\rm eff}(\mathbf{r}) - \mu\})$ is the position-dependent fugacity (μ is the condensate chemical potential). The particle coordinates, as well as the condensate density, are then rotated through an angle $2\theta_0$ about the y axis relative to the trap potential $V(\mathbf{r})$.

Starting with these initial conditions, quadrupole moments can be calculated separately for the condensate ($Q_c(t) = \int d\mathbf{r}\, xz n_c$) and thermal cloud ($\tilde{Q}(t) = \sum_{i=1}^{\tilde{N}} x_i z_i$). To make contact with experiment we define a rotation angle for each component, $\theta_\alpha(t) = Q_\alpha(t)/Q_\alpha^0$, where $Q_\alpha^0 = \langle x^2 - z^2\rangle_\alpha^0$ is the equilibrium quadrupole moment of the α-th component [17]. For a pure condensate ($T = 0$) consisting of $N = 2\times 10^4$ atoms, the quadrupole moment is found to oscillate with almost constant amplitude (where small fluctuations arise from weak excitation of other condensate modes) at a single frequency of $\omega_{sc} = 2.9886\omega_\rho$, which is about 1.5% larger than the Thomas-Fermi result $\omega_{sc} = (\omega_\rho^2 + \omega_z^2)^{1/2}$ [2] due to finite number effects. Above T_c the Bose gas oscillation exhibits two frequencies with approximately equal amplitudes. Our simulations yield frequencies that are very close to those found experimentally and predicted analytically: $\omega_\pm = |\omega_\rho \pm \omega_z|$. In addition, the thermal cloud oscillation is weakly damped by C_{22} collisions, over a timescale which is similar for both modes and is of the order of several collision times.

Below T_c, our simulations describe the dynamics of both components. For most temperatures we find that the condensate and thermal cloud modes are essentially excited independently, indicating that the two components are only weakly coupled. Nevertheless, the condensate oscillation experiences significant damping from interactions with the thermal component. To quantify the damping rate and frequency of the condensate mode, the data is fit to a single exponentially-decaying sinusoidal

function in order to make contact with the experimental analysis [3]. Fig. 1 shows results for the condensate mode as a function of temperature, for a fixed total number of atoms, $N = 5 \times 10^4$. To separate the effects of each term in the Boltzmann equation (2) on the dynamics, simulations are performed with no collisions, with only C_{22} collisions, and with both C_{12} and C_{22}. At low temperatures ($T < 0.6T_c^0$) we see that the damping is predominately due to collisionless Landau damping, where mean field interactions between the condensate and thermal atoms transfer energy from the collective mode to single particle excitations. When C_{22} collisions are included, an increase in damping is observed. These collisions can only affect the condensate indirectly through their equilibrating effect on the nonequilibrium distribution of thermal atoms. The C_{12} term leads to additional damping at low T by further promoting the equilibration of the condensate and thermal cloud. This source of damping is comparable in magnitude to that of the C_{22} collisions but is small compared to Landau damping, in agreement with a previous study of collective modes under the assumption of a static thermal cloud [18]. The effect of C_{12} collisions can also be inferred by monitoring the number of condensate atoms as a function of time. Since the initial angular displacement of the cloud increases its total energy, the gas must equilibrate to a higher final temperature with a corresponding reduction in the condensate number. This is seen in the simulations.

At higher temperatures ($T > 0.6T_c^0$), collisional effects increase in importance, but the situation becomes more complicated as T_c^0 is approached. The more massive thermal cloud begins to drive the condensate at its own scissors mode frequencies, and as a result, a single damped sinusoid is a poor fit to the theoretical data in this regime. Effectively, the condensate oscillations are sustained over longer times and the damping appears to saturate.

There are also observable effects on the condensate mode frequency. In the collisionless limit, we see from Fig. 1(a) that the frequency at first increases with increasing temperature as a result of the decreasing number of condensate atoms (i.e., the frequency shifts away from the TF limit). This trend is reversed by collisions, as well as at higher temperatures where the thermal cloud becomes significant. Since the condensate tends to drag part of the thermal cloud along with it, its effective inertia is increased. One would therefore expect a lowering of its normal mode frequency, as observed.

Use of evaporative cooling in the actual experiments [3] meant that the total number of atoms varied with temperature from $N \simeq 2 \times 10^4$ at low T to $N \simeq 10^5$ close to T_c^0. Since a small but significant dependence on number is found in our full simulations, we have taken this variation into account in our comparison with experiment. Our results in Fig. 2 are in very good agreement with experiment for $T < 0.8T_c^0$ but deviate from experiment in both frequency and damping at the three highest temperatures. However the experimental error bars are particularly large for these points, which may reflect difficulties in extracting values of the damping rate and frequency from fits to the data over a limited timescale. We note that three damped sinusoids are needed to fit the theoretical data in this regime, as the condensate is strongly coupled to the thermal cloud. In addition, we do not see a condensate at the highest temperature point ($T \simeq T_c^0$), which may indicate systematic errors in the experimental temperature scale or possibly limitations of the semiclassical approximation.

A quantity of considerable interest is the quadrupole response function $\chi''(\omega)$, which physically describes the energy absorption of each mode under a harmonic perturbation. Zambelli and Stringari [17] demonstrated that this can be related to the moment of intertia of the system, Θ, by the expression

$$\frac{\Theta}{\Theta_{\rm rigid}} = (\omega_z^2 - \omega_\rho^2)^2 \frac{\int {\rm d}\omega\, \chi''(\omega)/\omega^3}{\int {\rm d}\omega\, \chi''(\omega)\, \omega}, \qquad (4)$$

where $\Theta_{\rm rigid}$ is the moment of inertia of the corresponding rigid body. For a sudden rotation of the trap, $\chi''(\omega) \propto \omega\, \Re\{Q(\omega)\}$, where $Q(\omega)$ is the Fourier transform of the time-dependent quadrupole moment. We extract this quantity by fitting three damped sinusoids to the calculated total quadrupole moment. Fig. 3 shows results as a function of temperature. At lower temperatures, the condensate mode is dominant and $\chi''(\omega)$ exhibits a single peak. For very low T the thermal cloud is in fact strongly coupled to the condensate, and oscillates at the condensate frequency with a small phase shift that accounts for condensate damping. However, as the temperature is raised, the strength of the condensate mode diminishes, and the spectral density is dominated by the two thermal cloud modes at $\omega_\pm$, as would be expected for $\Theta \simeq \Theta_{\rm rigid}$ [17]. In contrast, the small T behavior is consistent with a superfluid moment of intertia, $\Theta_{\rm sf} < \Theta_{\rm rigid}$. In principle, one could calculate the moment of inertia over the entire temperature range using (4). However, the damped nature of the modes leads to Lorentzian spectral densities for which the required frequency moments are undefined. Nevertheless, one can see qualitatively that $\Theta_{\rm sf} < \Theta < \Theta_{\rm rigid}$ in the intermediate region.

To summarize, we have simulated the scissors modes in a finite-temperature Bose gas using a coupled FFT/Monte-Carlo scheme. Our approach takes into account fully the dynamical mean fields acting between the condensate and thermal cloud as well as all collisional processes that are physically relevant. We find very good agreement with experiment over a wide range of temperatures, with only minor discrepancies near to T_c^0 where both theory and experiment are more difficult to analyze quantitatively. These same methods can be used to study other collective modes, as well as problems such as condensate growth.

We acknowledge financial support from NSERC of Canada, and the use of the HPCVL computing facilities at Queen's. We thank A. Griffin, J. Williams and T.

Nikuni for valuable discussions, and O. Maragò and C. Foot for providing experimental data. BJ would also like to thank C. Adams and J. McCann for their help and support over an extended period.

[1] O. M. Maragò, S. A. Hopkins, J. Arlt, E. Hodby, G. Hechenblaikner, and C. J. Foot, Phys. Rev. Lett. **84**, 2056 (2000).
[2] D. Guery-Odelin and S. Stringari, Phys. Rev. Lett. **83**, 4452 (1999).
[3] O. M. Maragò, G. Hechenblaikner, E. Hodby, and C. J. Foot, Phys. Rev. Lett. **86**, 3938 (2001).
[4] F. Dalfovo, S. Giorgini, L. P. Pitaevskii, and S. Stringari, Rev. Mod. Phys. **71**, 463 (1999).
[5] D. A. W. Hutchinson, E. Zaremba, and A. Griffin, Phys. Rev. Lett. **78**, 1842 (1997).
[6] R. J. Dodd, M. Edwards, C. W. Clark, and K. Burnett, Phys. Rev. A **57**, R32 (1998).
[7] E. Zaremba, T. Nikuni, and A. Griffin, J. Low Temp. Phys. **116**, 277 (1999).
[8] S. A. Morgan, J. Phys. B **33**, 3847 (2000); S. Giorgini, Phys. Rev. A **61**, 063615 (2000).
[9] R. Walser, J. Williams, J. Cooper and M. Holland, Phys. Rev. A **59**, 3878 (1999); M. Imamovic-Tomasovic and A. Griffin, J. Low Temp. Phys. **122**, 617 (2001).
[10] Energy conservation and significant gains in stability are realized using a second-order approximation for the evolution operator: $\Phi(t+\Delta t) = e^{-i\tilde{H}\Delta t}\Phi(t)$, where $\tilde{H}(t) = [3H(t) - H(t-\Delta t)]/2$. Typically $\omega_\rho \Delta t = 1.5\times 10^{-3}$, while a 3D spatial grid of $64\times 64\times 32$ points is utilized.
[11] H. Wu, E. Arimondo, and C. J. Foot, Phys. Rev. A **56**, 560 (1997).
[12] G. A. Bird, *Molecular Gas Dynamics and the Direct Simulation of Gas Flows* (Oxford University Press, Oxford, 1994).
[13] H. Yoshida, Celest. Mech. Dyn. Astron. **56**, 27 (1993).
[14] R. W. Hockney and J. W. Eastwood, *Computer simulations using particles* (McGraw-Hill, New York, 1981).
[15] B. Jackson and C. S. Adams, Phys. Rev. A **63**, 053606 (2001).
[16] B. Jackson and E. Zaremba (in preparation).
[17] F. Zambelli and S. Stringari, Phys. Rev. A **63**, 033602 (2001).
[18] J. E. Williams and A. Griffin, Phys. Rev. A **63**, 023612 (2001).

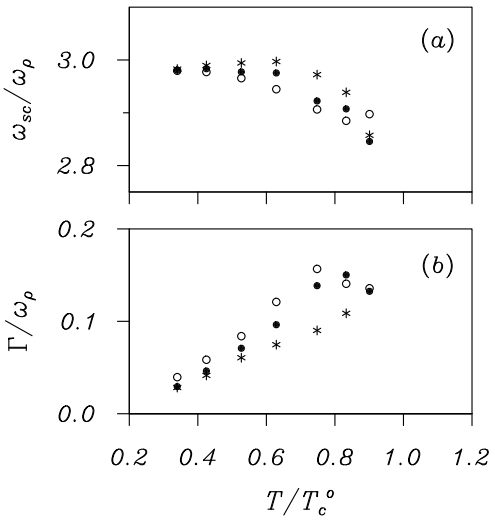

FIG. 1. Frequency (a) and damping rate (b) of the condensate scissors mode as a function of temperature for $N = 5\times 10^4$ total particles. Note that the temperature is normalized by the transition temperature of the ideal gas, T_c^0. Each plot shows the effect of inclusion of each term in the kinetic equation (2): the free-streaming operator alone ($*$); the free-streaming and C_{22} terms ($\bullet$); and all terms ($\circ$).

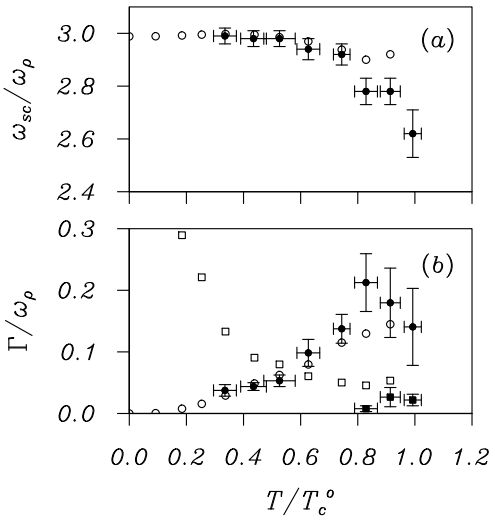

FIG. 2. Frequency (a) and damping rate (b) of the scissors modes for a variable total number of atoms, intended to simulate the experimental parameters. The condensate mode is indicated by open (theory) and solid (experiment) circles. The open squares in (b) show the calculated average damping rate of the two thermal cloud modes, while the solid squares are the corresponding experimental values.

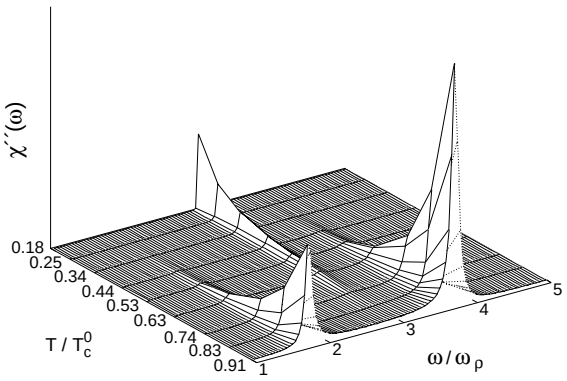

FIG. 3. Quadrupole response function $\chi''(\omega)$ for the system, as a function of frequency and temperature. The parameters match those in Fig. 2.